American Journal of Psychiatry and Neuroscience
2022; 10(2): 63-76
http://www.sciencepublishinggroup.com/j/ajpn
doi: 10.11648/j.ajpn.20221002.12
ISSN: 2330-4243 (Print); ISSN: 2330-426X (Online)

Exploring the Secretome's Biomarker and Analgesic Potential

Megan Rose Hershfield[1], Misty Marie Strain[1], Roger Chavez[1], Michaela Rae Priess[1], Alberto Mares[1], Aarti Gautam[2], George Dimitrov[3], Ruoting Yang[2], Alex Valdez Trevino[1], Col Kenney Wells[1], Col Thomas Stark[1], Rasha Hammamieh[2], John Leo Clifford[1], Natasha Marie Sosanya[1, *]

[1]Pain and Sensory Trauma, US Army Institute of Surgical Research, JBSA Fort Sam Houston, USA

[2]Medical Readiness Systems Biology Branch, Walter Reed Army Institute of Research, Silver Spring, USA

[3]The Geneva Foundation, Tacoma, USA

Email address:

Natasha.m.sosanya.ctr@mail.mil (N. M. Sosanya), Natasha_sosanya@yahoo.com (N. M. Sosanya)

[*]Corresponding author

To cite this article:

Megan Rose Hershfield, Misty Marie Strain, Roger Chavez, Michaela Rae Priess, Alberto Mares, Aarti Gautam, George Dimitrov, Ruoting Yang, Alex Valdez Trevino, Col Kenney Wells, Col Thomas Stark, Rasha Hammamieh, John Leo Clifford, Natasha Marie Sosanya. Exploring the Secretome's Biomarker and Analgesic Potential. *American Journal of Psychiatry and Neuroscience*. Vol. 10, No. 2, 2022, pp. 63-76. doi: 10.11648/j.ajpn.20221002.12

Received: April 1, 2022; **Accepted**: April 20, 2022; **Published**: May 10, 2022

Abstract: Diagnostic and prognostic biomarkers of nerve injury and/or pain as well as improved pain therapeutics are needed, both on the battlefield to treat injured Service Members and in the civilian sector. Our previous research indicates that there are several differentially expressed (DE) extracellular vesicle-derived microRNAs (EV-miRNAs) isolated from rat plasma following spinal nerve ligation (SNL). As such, EV-miRNAs hold promise as biomarkers and therapeutic targets. The secretome contains biological mediators, including EVs, which are released into the extracellular space. In this study we focus on evaluating EV-non-coding RNAs (ncRNAs), examine effects of SNL on key protein expression in the prefrontal cortex (PFC), and test the secretome's analgesic properties. To accomplish these goals, anesthetized male Sprague Dawley rats underwent SNL and nociceptive behavior measurements, plasma collection followed by EV RNA isolation, small RNA sequencing, and analysis. Expression of several key proteins in the PFC was determined by Wes/Jess analysis. The secretome bath was applied directly to the ligated nerve and the paw withdrawal threshold (PWT) was measured. We identified differences in several classes of ncRNAs such as piRNAs, snoRNAs, and snRNAs post-SNL. Levels of phosphorylated forms of P70S6K and ERK1 were increased in the dorsal PFC at 15 days post-SNL. Bath application of the secretome directly to the ligated nerve resulted in recovery of the reduced PWT (increased mechanical sensitivity) that is induced by SNL. Here, we have identified specific EV-ncRNAs that could contribute to the formation of pain. Furthermore, we have evaluated a novel product for analgesic efficacy that could function to exploit the underlying mechanisms that contribute to pain development, thus reducing acute pain. This is key in treating Service Members on the battlefield in order to prevent pain chronification.

Keywords: Secretome, Nociception, Extracellular Vesicles, Analgesia, Spinal Nerve Ligation, Non-coding RNA

1. Introduction

During Operation Enduring Freedom (OEF) and Operation Iraqi Freedom (OIF), advances in battlefield emergency medical care, protective body armor, and rapid evacuation from far forward locations to higher level medical settings has resulted in greater than 90% survival rates from battlefield injuries. Such injuries have produced an unprecedented incidence of severe pain amongst active-duty service members and veterans. Injury and/or pain biomarkers as well as treatments that are conducive to battlefield use are needed. Injury biomarkers have the potential to effect triage and evacuation decisions. This will become even more relevant in future conflicts with predicted longer evacuation times.

Other fields have identified and used disease biomarkers for years. However, prognostic and diagnostic biomarkers for pain are limited. This restricts our treatment options to be based on subjective and potentially inaccurate descriptions of pain. In terms of Military and battlefield usefulness, this potential pain diagnostic test could (1) improve return to combat time after injury, (2) quantitatively measure pain to augment the Visual Analog Pain Scale, (3) measure pain intensity in a non-communicative patient, and (4) provide information that enables more precise analgesic dosing [1]. Physicians welcome such pain biomarkers, which enable proper diagnosis and implementation of the best treatment plan. Improper diagnoses can lead to unpleasant outcomes including mismanaged drug use and lack of confidence in the patient-doctor relationship.

Previously, we have shown that circulating extracellular vesicles (EVs) released post-nerve injury are deficient in miRNAs that suppress inflammatory mediators of pain [1]. Specifically, we found that 22 and 74 miRNAs at day 3 and 15, respectively, and 33 miRNAs at both days 3 and 15 were uniquely differentially expressed (DE) between sham and nerve injured rats [1]. The key findings from the previous research was (1) the majority of the DE EV-miRNAs, which normally function to suppress inflammation, were downregulated and (2) several of the plasma derived DE EV-miRNAs reflect previously observed changes in the injured L5 nerve suggesting that these are potential nerve injury biomarkers [1]. The goals of the current research is to expand on our previous findings by determining if further changes in other non-coding RNAs (ncRNA) is observed, evaluate changes in cortical proteins that contribute to pain, and evaluate the secretome for its analgesic potential.

EVs are membrane bound particles released by cells that retain the phenotype and molecular signature of the cell type of origin (e.g., protein, mRNA, ncRNA, DNA and lipids) [2]. EVs and their content serve as promising biomarkers and treatments for pain, tissue injury, and a number of other medical conditions [3-6]. EVs are abundant in biological fluids and include both exosomes and microvesicles, which are capable of inducing significant genotypic/phenotypic changes at the receiving cell [7]. Besides transporting characteristic proteins and lipids, EVs package a wide range of RNA species varying in size and function.

ncRNAs which include PIWI-interacting RNAs (piRNAs), small nucleolar RNAs (snoRNAs), small nuclear RNAs (snRNAs), long noncoding RNAs (lncRNAs), and miRNAs are known to make up 99% of total RNA content and are emerging as potential biomarkers for disease [8]. Currently, the exact roles and molecular mechanisms of action of many classes of ncRNAs have not been fully explored. PiRNAs, 24–31 nucleotides (nt), modulate signaling pathways and have been examined as potential biomarkers for tumorigenesis and cancer prognosis [9]. SnoRNAs are 60–300 nt and function in ribosome biogenesis, serving as guides for the site-specific modification of ribosomal RNA (rRNA) [10]. SnRNAs, ~150 nt, are the component parts of the spliceosome responsible for the removal of non-coding introns from precursor mRNA. Aberrations in snRNA splicing regulation has been linked to specific motor neuron diseases [11]. LncRNAs, more than 300 nt, have roles in both transcriptional and post-transcriptional regulation, [12] and have key implications in models of cancer [13] as well as inflammation [14]. The most studied EV ncRNAs are miRNAs which are ~22 nt and negatively regulate gene expression at protein level by either mRNA degradation or translational inhibition [15]. MiRNAs present in circulating EVs have been linked to neurodegenerative disorders and pain [16-19] and have been proposed as biomarkers for cancer diagnostics, [20-22] and for neuropathic injury [1].

EV-ncRNAs make up a portion of the secretome, which is defined as all the elements that a cell releases into the extracellular space, whether *in vitro* or *in vivo*, and can be divided into the soluble fraction containing proteins and cytokines and the vesicular fraction containing exosomes, microvesicles and apoptotic bodies [23-28]. The therapeutic application of the secretome of mesenchymal stromal cells (MSCs) showed regenerative potential in a model of heart infarct [29] and increased the survival and viability of different neuronal and glial cell populations *in vitro* [30]. Due to the MSC secretome's neuroprotective effects, it has also been evaluated as a pain therapeutic. In a mouse model of diabetic neuropathy, the secretome from human adipose MSCs was administered to diabetic neuropathic mice resulting in reversal of mechanical allodynia and thermal hyperalgesia [31]. Two other studies utilized human bone-marrow-derived MSC secretome which suppressed nociceptive behavior in mouse models of osteoarthritis [32] and partial sciatic nerve ligation [33], highlighting their therapeutic potential.

Identifying EV-contained ncRNA cargo from the secretome and evaluating their biomarker potential for neuropathic pain development is of importance. We have previously utilized a neuropathic pain model, spinal nerve ligation (SNL) in rats, to investigate EV-miRNAs contribution to pain development [1]. Several plasma derived EV-miRNAs were DE following injury. We hypothesize that EV containing not only miRNA but other classes of ncRNAs and their downstream targets could play a critical role not only in the progression from acute to chronic pain but also as targets of pain therapeutics [1]. For example, found in the secretome, vascular endothelial growth factor (VEGF) participates in the formation, growth and survival of new blood vessels [34-38]. In the nervous system, VEGF has been associated with neuroprotection through the VEGF receptor and MAPK/Erk1/2 signal transduction pathways [39] and the reorganization of the spinal motor network after spinal cord injury (SCI) [40]. Our recent findings showed a downregulation of the EV-miRNAs modulating these pathways.

In the present study we have identified several other EV ncRNA biomarkers that could contribute to nociceptive behavior, have determined if key protein targets are altered in the brain after injury, and have tested the secretome's analgesic properties.

2. Materials and Methods

2.1. Animals

Forty-nine 7- to 8-week-old adult male Sprague-Dawley rats, (Charles River Laboratories, USA), were used in this study. Upon arrival, rats were quarantined for 3 days and then pair housed in cages with a 12 hours light/dark cycle (Light: 6 AM − 6 PM) with ad libitum access to food and water. Following a week of acclimation to the facility, experimental procedures began. Research was conducted in compliance with the Animal Welfare Act, the implementing Animal Welfare Regulations, and the principles of the Guide for the Care and Use of Laboratory Animals. The Institutional Animal Care and Use Committee approved all research conducted in this study. The facility where this research was conducted is fully accredited by the AAALAC. The minimal number of animals were used to conduct this study.

2.2. Experimental Groups

All experiments were performed in a blinded fashion. Two distinct rat groups were used to examine the spinal nerve ligation (SNL) effects on EV small RNA cargo [1]. Mechanosensitivity testing was performed and published previously [1]. Sham surgery control (n=6) made up group 1. SNL surgery (n = 6) made up group 2. We isolated the prefrontal cortex from 4 rats per group at day 15 post-SNL to examine changes in key protein targets. We used a separate group of rats to isolate the prefrontal cortex from 4 rats per group at day 3 post-SNL. The sham group was exposed to all the same conditions as the SNL group minus the L5 ligation [1]. In a separate experiment, observing the same design, we studied the effects of a secretome product on nociceptive behavior (n=6 per group).

2.3. Spinal Nerve Ligation (SNL) Model for EV ncRNA Evaluation

Each rat was completely anesthetized (4% isoflurane in oxygen) followed by anesthesia maintenance using 2.5% isoflurane in oxygen provided through a nose cone [1]. Two subcutaneous injections of 0.05 mg/kg buprenorphine were administered; one immediately prior to surgery and one 8 to 12 hours post-surgery for analgesic purposes [1]. The spinal nerve ligation procedure was performed as described previously [1].

2.4. Liquid Biopsy Method and EV RNA Extraction

A 21G butterfly needle (BD 367281, minus the plastic tubing and luer adapter) was used to draw blood from the tail vein at each interval [1]. The total withdrawn blood sample was ~700 µl per rat (7% circulating blood volume [CBV]) per interval [1]. Throughout this process, the rats were placed in a mechanical restrainer based on their weight (Harvard apparatus 52−0494 or 52−0486) [1]. The tail was placed in 42°C water to expand the blood vessels preceding collection [1]. 2% chlorhexidine antiseptic solution was applied to the tail. Blood was collected in ethylenediaminetetraacetic acid (EDTA) tubes (BD microtainer 365974), centrifuged twice at 4°C at 1000xg for 15 minutes [1]. The clear plasma supernatant, following centrifugation, was isolated and stored at -80°C until downstream handling [1].

The miRCURY exosome isolation kit − serum and plasma (Qiagen cat# 76603) was utilized to isolate EVs with a starting material of 250 µl plasma per sample [1]. The miRNeasy serum/ plasma advanced kit (Qiagen cat# 217204), following the manufacturer's directions, was then used to isolate the RNA [1]. Approximately 100 ng of total RNA was isolated from each sample. RNA was deposited at -80°C prior to shipment to the collaborator's site for further analysis.

2.5. Microfluidic Resistive Pulse Sensing (MRPS)

Plasma EVs isolated from both sham and SNL animals were sent to Spectradyne for MRPS nanoparticle analysis and characterization of EV particle size and concentration.

2.6. Brain Microdissection

Following the last behavioral tests, the rats were humanely euthanized by decapitation in accordance with USAISR IACUC Policy: Use and Maintenance of Guillotine's for Rodents [41]. Rats, minus analgesics/anesthetics, were restrained in a plastic Decapicone and were decapitated using a guillotine (Harvard Apparatus) by skilled personnel [41]. This technique permits isolation of whole brain tissue minus chemical adulteration. The brains were instantly removed, flash-frozen in liquid nitrogen and deposited at − 80°C pending usage [41]. Brain microdissection was performed as described previously [41]. Our team has previously evaluated mRNA isolated from specific brain regions, including the PFC, post nerve-injury (unpublished data, article in prep). The PFC shows specific changes in key signaling pathways associated with pain.

2.7. Wes and Jess Protein Detection

The Wes™ and Jess™ system utilizes Separation Modules for electrophoresis gel preparation, and specific modules for gel detection of specific antibody labeled targets and then a Fluorescent Substrate for site detection once exposed. When the gel has completed its separation sequence, the Wes™ and Jess™ system observes a selected excitation capture for a designated period of exposure, and finally data are collected as pixels depicting the separated protein sizes and concentration through the system software. Phosphorylated-ERK ½ (LSbio C97127), MAPK14 (LSbio LS-B1643), phosphorylated P70S6K (LSbio C117452), and total protein expression was determined by Wes™ and Jess™ analysis ProteinSimple SM-W004 (12-230 kDa Separation Module), DM-001 (Anti-rabbit detection module), DM-TP01 (Total protein detection module); following the manufacturer's directions. Lysate was used at a final protein concentration of 0.2 mg/ml. Bicinchoninic acid (BCA) (ThermoFisher) analysis was conducted to measure protein concentration and all measures were taken to load equal amounts of total protein per sample onto the plate. The primary antibody was used at a 1:50 dilution. All experimental targets were

normalized to total protein expression, which served as the loading control [42]. Data examination was completed using the Wes/Jess and ImageJ software.

2.8. Spinal Nerve Ligation Model for Secretome Product Evaluation

The SNL procedure was conducted in a similar manner as was previously described [1]. However, buprenorphine injections were not performed as they would interfere with the evaluation of the secretome product that was applied at the time of nerve injury. This product is derived from the cultured media released from mesenchymal stromal cells (MSC) and has potential neuroprotective and anti-inflammatory properties [43-47]. We obtained the secretome, termed Thera101, from Theratome Bio, Inc. Immediately following nerve injury, 350-450µl of secretome (1-2 mg/kg) was applied directly to the injured nerve. The secretome was allowed to bath the nerve for 1 minute prior to closing the wound. The secretome was applied directly after nerve injury for a few reasons including (1) our goal was to determine if the secretome can function as a nerve block, (2) to address whether the secretome application can block mechanosensitivity from forming and (3) because our lab conducts military research which is focused on acute pain and treatment application at the point-of-injury (POI). Sham+Saline, SNL+Saline, and SNL+Secretome surgeries were conducted in random order. Mechanosensitivity testing was performed at 0.5, 1 and 2 hrs. post-nerve injury.

2.9. Mechanosensitivity Assay

Three measurements were recorded for each left and right hind paw at baseline, 0.5, 1, and 2 hrs. post-nerve injury. Baseline recordings were acquired preceding the SNL injury [1]. Rats were rested at a minimum of 1 minute between each recording [1].

2.10. Statistical and Bioinformatics Analysis

A power analysis was performed prior to conducting the behavioral experiments. A sample size of 6 rats per treatment group and per time point was needed to determine statistical significance with a power (1-β) of 0.80, and a probability of a Type I error (α) of 0.05. These numbers resulted in 80% power for detecting a difference between the SNL and sham groups at each time point using two-way repeated-measures (RM) ANOVA.

For the molecular experiments, a sample size of 4 rats per treatment group and per time point was predicted to reach statistical significance with a power of 0.80 and $\alpha = 0.05$. These numbers resulted in 80% power for detecting a difference between rat groups using independent sample t-test.

The principal experimental results involved behavioral alterations and EV biomarker identities. Graph-Pad 7 (Graph Pad Software, Inc., La Jolla, CA) software was used to examine the behavioral figures. Data is conveyed as the mean ± standard error of the mean (SEM). To analyze changes in mechanical allodynia over a period of time, two-way RM ANOVA was utilized [1]. Bonferroni post-hoc test was performed to control the false discovery rate. P-values of $< .05$ were considered significant.

Samples from previously published manuscript [1] were used for ncRNA analysis. The raw BCL files were converted to fastq files during de-multiplexing with bcl2fasq (Illumina), followed by CLC genomic workbench version 20.0.4. Reads were trimmed for illumina adapter sequences and low quality reads were removed. Trimmed reads were mapped to rat mature and precursor miRNAs using the miRBase - Release 22.1. In addition, custom database for variety of ncRNA was generated by downloading published sequences from RNAcentral, a comprehensive database of ncRNA sequences [48]. Reads were annotated for matches against known ncRNAs related to Rattus norvegicus. The number of reads mapped to each ncRNA was counted, and then normalized to account for differences in sequencing depth by using counts-per-million (CPM-TMM adjusted). T-tests were used to compare the expression level between different groups. P-values of $< .05$ were considered significant. The final fold change values were given in log2 scale and the ncRNA with log2-fold change (log2FC) higher than 0.2 or less than −0.1 were designated as up-regulated and down-regulated, respectively.

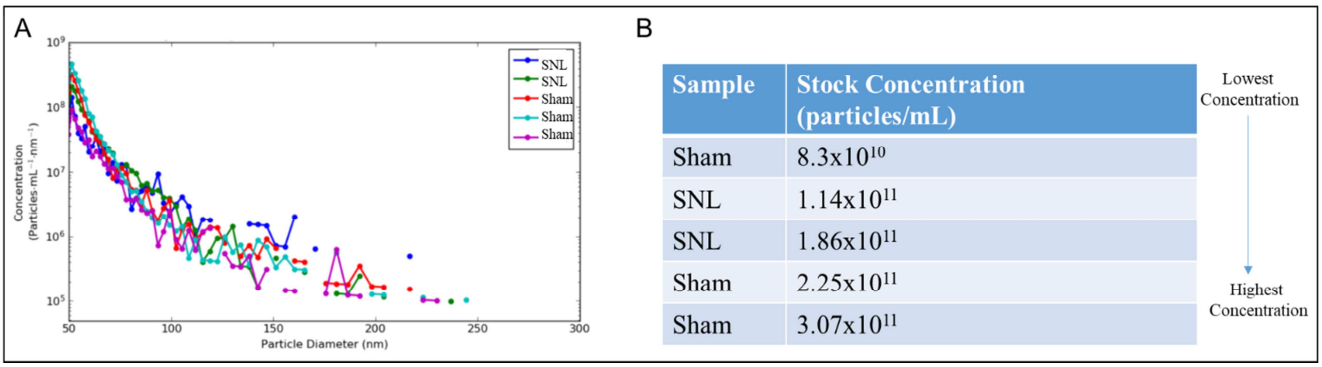

Sample	Stock Concentration (particles/mL)
Sham	$8.3x10^{10}$
SNL	$1.14x10^{11}$
SNL	$1.86x10^{11}$
Sham	$2.25x10^{11}$
Sham	$3.07x10^{11}$

Figure 1. *MRPS analysis revealed no significant difference in EV concentration or size between sham and SNL groups.*

A) Plasma derived EVs were not significantly different in concentration or particle diameter between the sham and SNL groups.
B) The number of EV particles/mL from the sham and SNL groups ranked from lowest to highest.

3. Results

3.1. Effects of SNL on EV Concentration and Size

MRPS analysis of plasma derived EVs following sham and SNL surgery revealed no significant difference in EV concentration or particle diameter between groups (Figure 1A-B).

These results are in agreement with our previous published research characterizing EVs isolated from plasma of non-injured rats as well as conform to literature describing EV concentration, size, and content [1].

3.2. Effects of SNL on EV RNA Content

EV-miRNAs were differentially expressed (DE) between SNL and sham groups at 3 and 15 days post-SNL [1]. An EV-miRNA is upregulated when the average expression level of SNL group is higher than that of sham group, and down-regulated when expression of SNL is lower than that of sham. Based on the potential contribution of ncRNAs to nerve injury and pain pathophysiology, the same core sequencing data was next analyzed for alterations in other ncRNAs, besides miRNAs. Specifically, lncRNA, piRNA, snoRNA, and snRNA were evaluated. 8 lncRNAs were DE at 3 and 15 days post-SNL (Figure A1). 36 piRNAs were DE at 3 and 15 days post-SNL injury (Figure 2). A majority of piRNAs that are upregulated or downregulated at day 3 compared to BL, appear to be oppositely regulated at day 15 (Figure 2). 18 snoRNAs are DE at days 3 and 15 post-SNL injury. The majority of DE snoRNAs are upregulated at both 3 and 15 days post-SNL (Figure 3A). Table A1 lists the DE EV snoRNAs using both the RNAcentral ID and correlating Ensembl ID. 19 snRNAs are DE at 3 and 15 days post-SNL (Figure 3B). At day 3, the majority of snRNAs are decreased whereas these same snRNAs are increased at day 15 (Figure 3B).

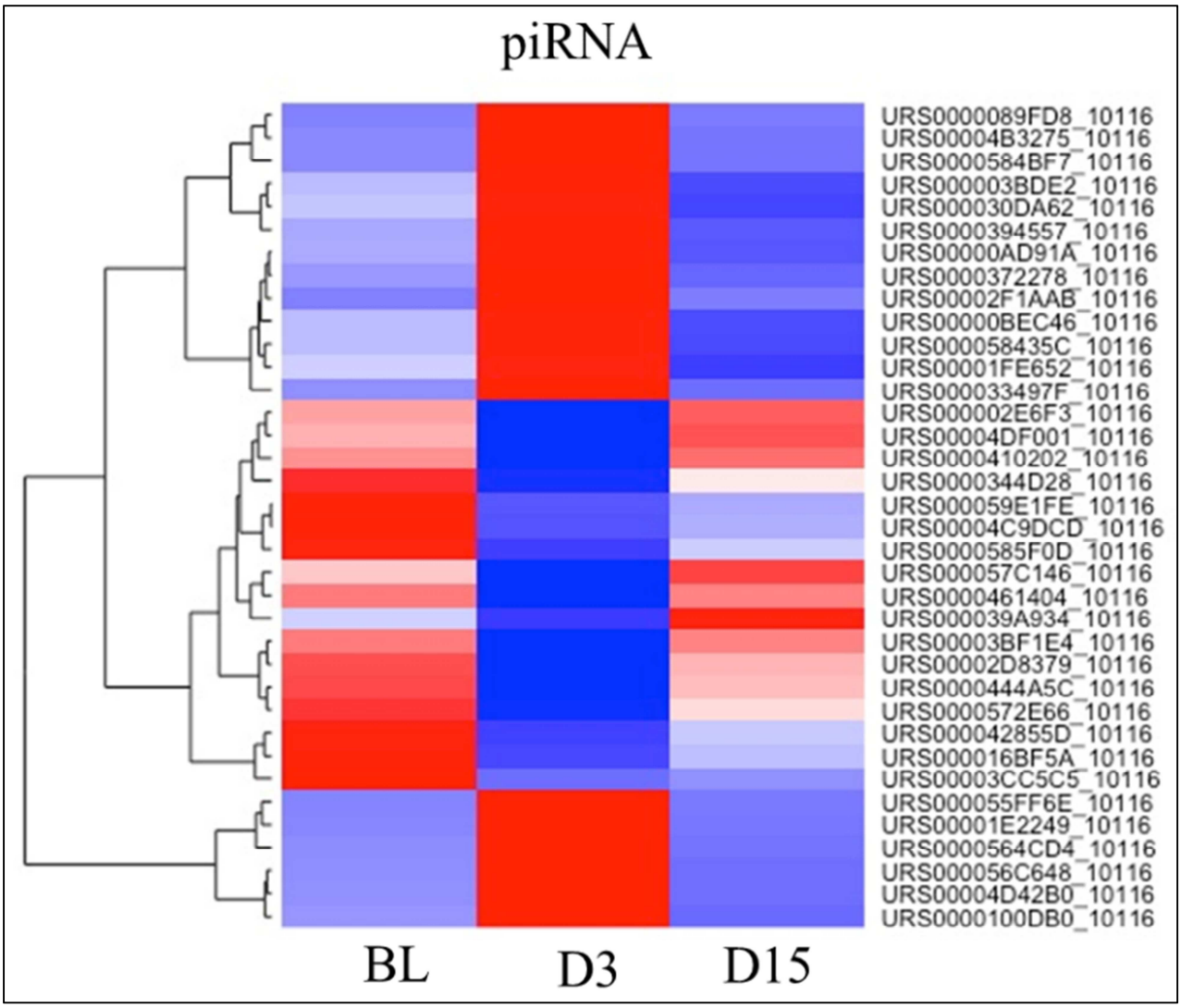

Figure 2. *Small RNA sequencing of nerve-injury induced EV RNAs revealed differentially expressed piRNAs.*

Heat map analysis revealed 36 piRNAs that were differentially expressed at days 3 and 15 post-SNL. A substantial percentage of the piRNAs that were up or downregulated at day 3 appeared to be oppositely regulated at day 15. Red: upregulated; blue: downregulated. N=6/group/timepoint.

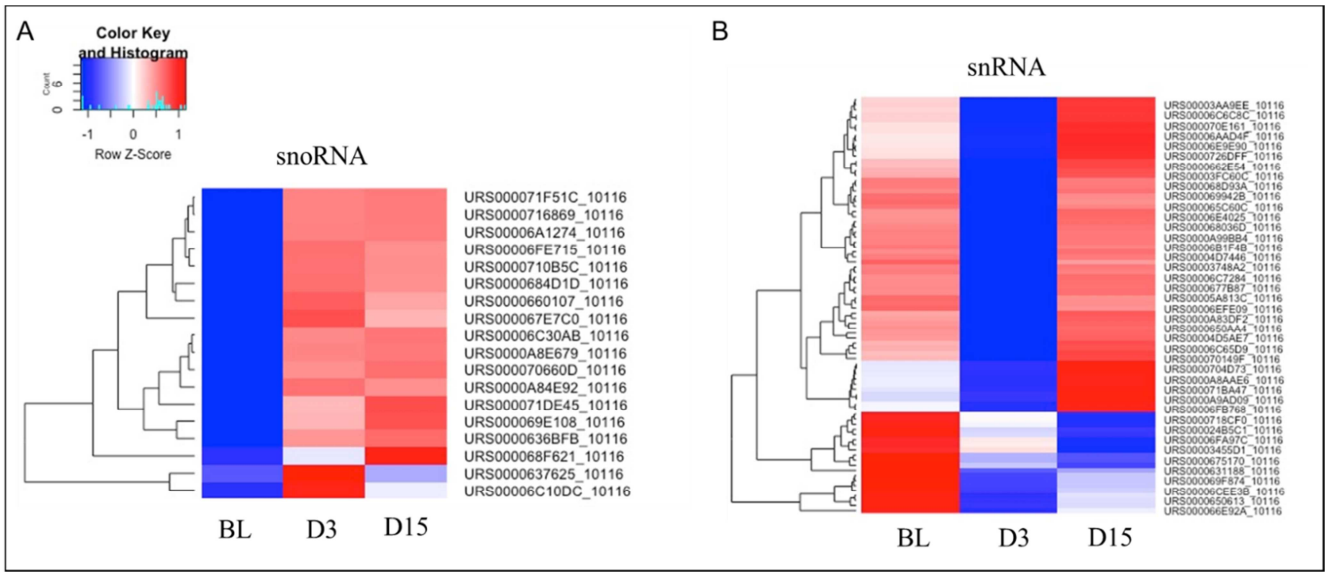

Figure 3. *Small RNA sequencing of nerve-injury induced EV RNAs revealed differentially expressed snoRNAs and snRNAs.*

A) Heat map highlighting 18 differentially expressed snoRNAs at days 3 and 15 post-SNL. The majority of these snoRNAs were upregulated. Red: upregulated; blue: downregulated. N=6/group/timepoint.

B) Heat map analysis revealed 16 snRNAs that were differentially regulated at days 3 and 15 post-SNL. The majority of these snRNAs were downregulated on day 3 whereas on day 15 they were upregulated. Red: upregulated; blue: downregulated. N=6/group/timepoint.

3.3. Expression of Pain Signaling Associated Proteins in the Dorsal PFC

We explored the expression profiles of key pain signaling associated proteins in the PFC. Due to their functional contribution to pain, the phosphorylation levels (indicating activation) of ERK1/2, MAPK, and P70S6K, were measured. No significant difference was observed between sham and SNL at day 3 post-SNL in the ipsilateral or contralateral dorsal PFC for p-ERK1/2, MAPK, and p-P70S6K (Figures 4-5). However, p-P70S6K were increased significantly in the contralateral PFC and p-ERK1 and p-P70S6K were significantly elevated in the ipsilateral PFC at day 15 post-SNL (Figures 6-7).

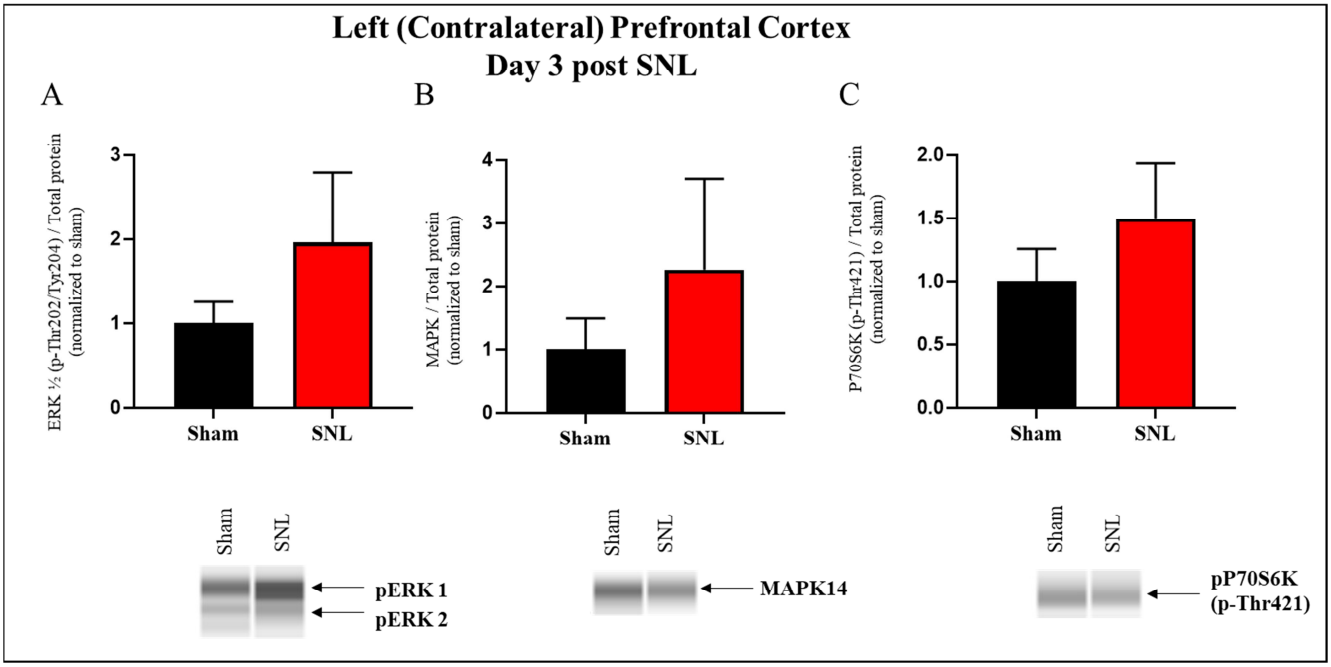

Figure 4. *Protein expression in the contralateral dorsal prefrontal cortex on day 3 post-SNL.*

(A-C) No significant differences were observed between the sham and SNL groups on day 3 post-SNL in the contralateral dorsal prefrontal cortex for p-ERK ½, MAPK, or p-P70S6K. Abbreviations: SNL, spinal nerve ligation. Error bars represent SEM. N=4/group.

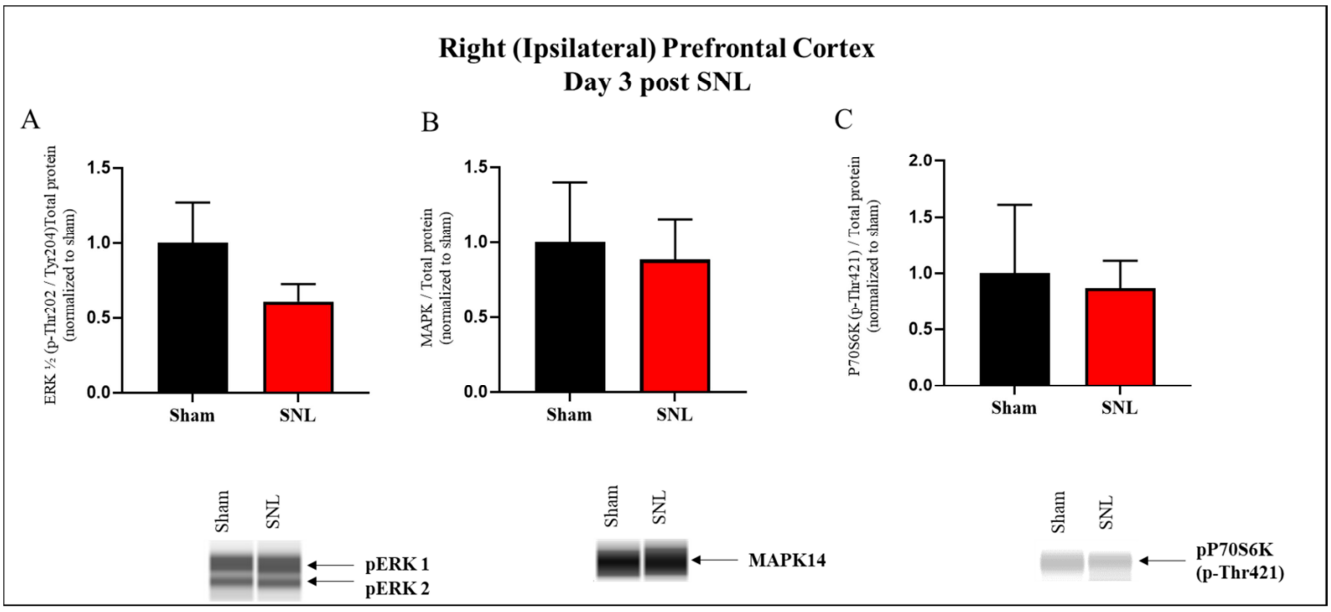

Figure 5. *Protein expression in the ipsilateral dorsal prefrontal cortex on day 3 post-SNL.*

(A-C) No significant differences were observed between the sham and SNL groups on day 3 post-SNL in the ipsilateral dorsal prefrontal cortex for p-ERK ½, MAPK, or p-P70S6K. Abbreviations: SNL, spinal nerve ligation. Error bars represent SEM. N=4/group.

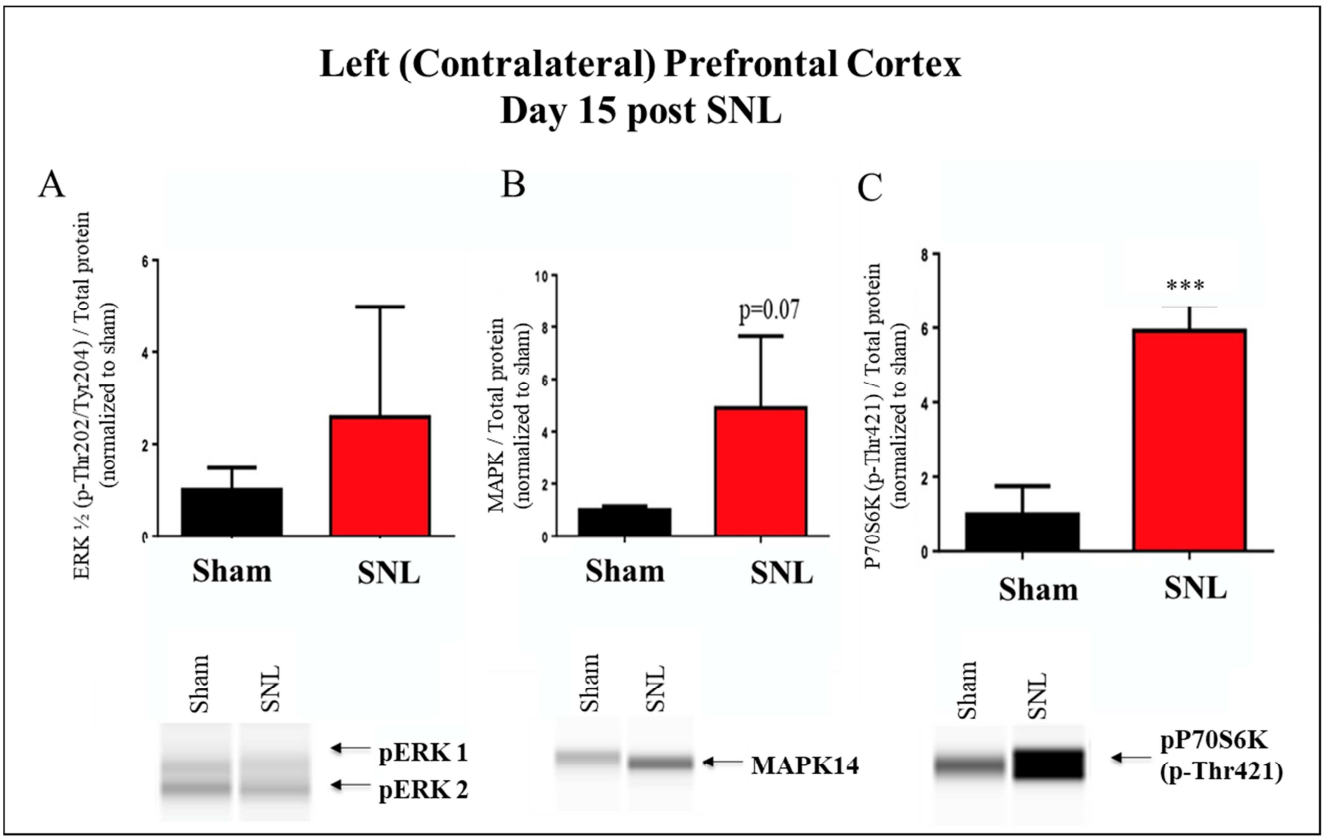

Figure 6. *Protein expression in the contralateral dorsal prefrontal cortex on day 15 post-SNL.*

A) No significant difference in p-ERK ½ expression was observed between the sham and SNL groups.
B) No significant difference in MAPK expression was observed between the sham and SNL groups.
C) The SNL group demonstrated a significant increase in p-P706SK expression. ***p<0.001, T-test. Error bars represent SEM. N=4/group.

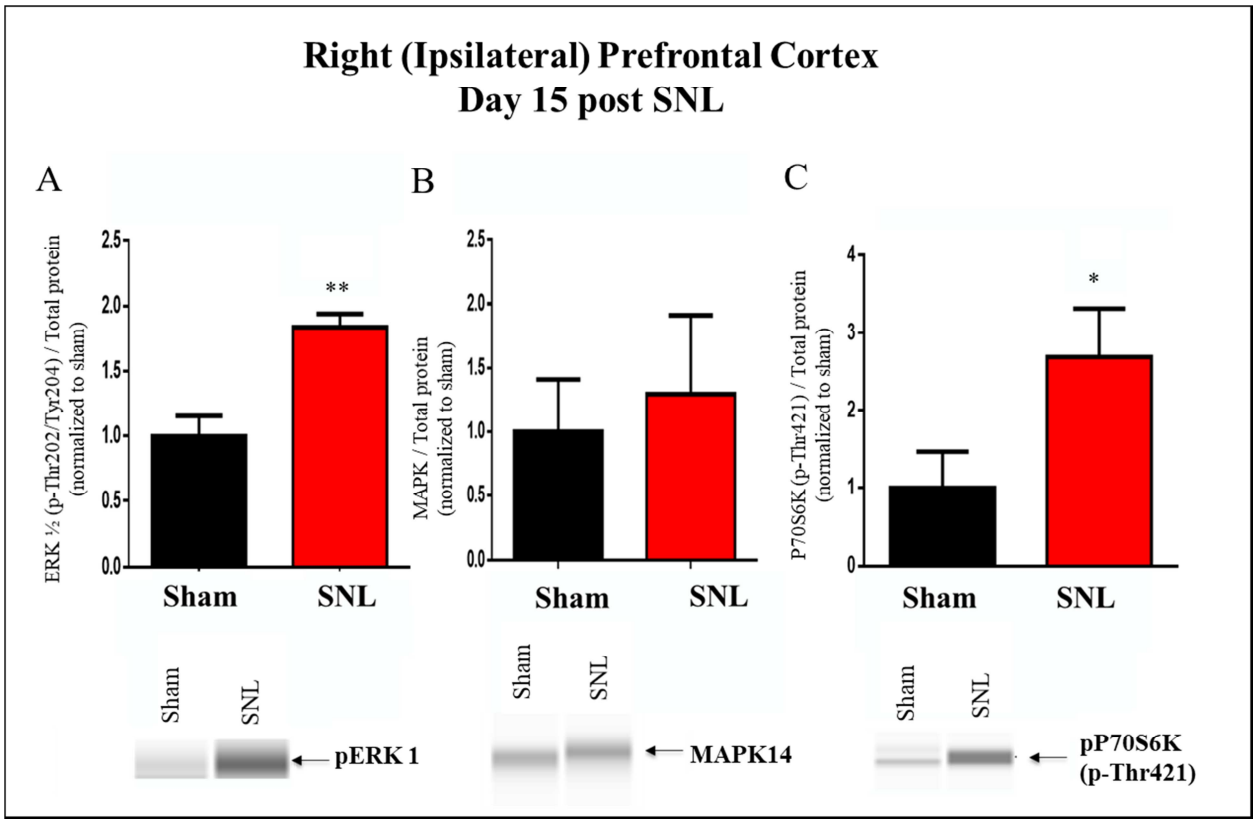

Figure 7. *Protein expression in the ipsilateral dorsal prefrontal cortex on day 15 post-SNL.*

A) The SNL group demonstrated a significant increase in p-ERK ½ expression. **p<0.01, T-test.
B) No significant difference in MAPK expression was observed between the sham and SNL groups.
C) The SNL group demonstrated a significant increase in p-P706SK expression. *p<0.05, T-test. Error bars represent SEM. N=4/group.

3.4. Effects of the Secretome on PWT Post-SNL Injury

Figure 8A is a timeline of the experimental procedure. SNL injury resulted in a reduction of the PWT at 1 and 2 hrs. post-surgery (Figure 8B). There was no significant difference between Sham+ SALINE and SNL+ SALINE at 30 min. post-injury. This may potentially be due to the rat still recuperating from anesthesia. Bath application of the secretome directly to the injured nerve resulted in blockage of the injury-induced nociceptive behavior (Figure 8B).

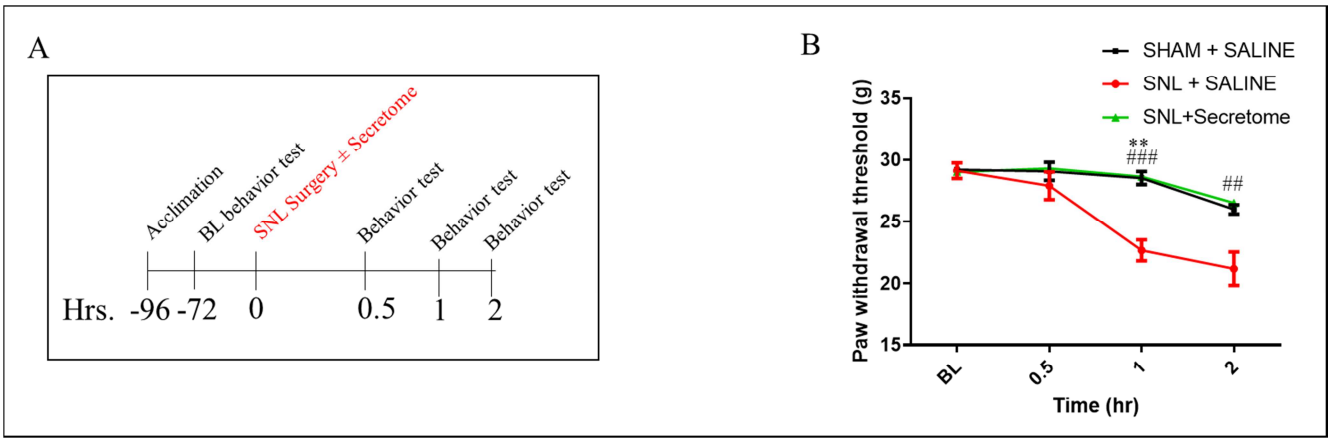

Figure 8. *Secretome application resulted in recovery of SNL-induced nociceptive behavior.*

A) Schematic representation of the experimental design and timeline.
B) At 1 and 2 hours post-injury, SNL resulted in a reduction of the PWT. SNL injury, followed by the application of the secretome, resulted in the recovery of PWT at 1 and 2 hours post-injury. #: compare SNL+SALINE (SA) to SNL+Secretome, *: compare SNL+SALINE to SHAM+SALINE. **p<0.01; ###p<0.001; ##p<0.01, RM ANOVA and Bonferroni post-hoc test. Error bars represent SEM. N=6/group.

4. Discussion

The hypotheses that are explored here were a direct result of our previously published research which evaluated EV-miRNA content post-nerve injury. In that work, the majority of the identified EV-miRNAs were downregulated and normally functioned to regulate inflammatory pathways [1]. We were interested in expanding our analysis to other ncRNA species and therefore mined the sequencing data for alterations in piRNA, snoRNA, snRNA, and lncRNA. Information about the miRNA and protein expression patterns in the brain post-nerve injury is lacking. Current work from our team is analyzing specific brain regions for changes in miRNA expression post-SNL.

Here, we have found that small ncRNAs (i.e. piRNA, snoRNA, snRNA, lncRNA) are present and altered post-nerve injury in plasma derived EVs. Furthermore, key pain signaling associated proteins are upregulated and activated in the prefrontal cortex at 15 days post-nerve injury. These targets (P70S6K and ERK1) are known to be important in the formation of neuropathic pain. Additionally, we evaluated the secretome for its analgesic potential. Direct secretome administration to the injured nerve blocked the reduced PWT caused by SNL. Future work will evaluate the secretome utilizing additional tests including the Mechanical Avoidance Conflict System (MACS) and gait analysis as well as in rodent models of inflammatory pain.

There is very limited literature on the role of snoRNAs, piRNAs, and snRNAs in neuropathic pain. Instead, the snoRNAs, SNORD50B, SNORA3, and U3 have been implicated in animal models of cancer [49-52]. Additionally, SNORA73 may have a role in ovarian function [53] and EV derived SNORD115 may function as a diagnostic biomarker of Alzheimer's disease [54]. The Ingenuity pathway analysis (IPA) bioinformatics analysis platform had limited information on the identified EV ncRNAs. Specifically, only SNORD50B was implicated in specific disease functions and SNORD71 and SNORA3 were mapped to known signaling pathways (Figure A2). While limited information exists regarding EV piRNA function in neuropathic pain, piRNAs have been identified in the central nervous system, [55] evaluated in a rat model of nerve injury [56] and patients with rheumatoid arthritis (RA) or osteoarthritis (OA) [57]. One manuscript has revealed that spinal piR-DQ541777 contributes to the formation of neuropathic pain in the chronic constriction injury (CCI) model [58]. There is very little, if any, information on the role of EV snRNA in neuropathic pain. However, snRNAs are abundant in EVs and may function as cancer biomarkers [59]. Unlike piRNAs, snoRNAs, and snRNAs, multiple studies have evaluated lncRNAs in animal models of neuropathic pain. Several studies have analyzed lncRNA expression in the spinal cord or dorsal root ganglion in rodent models of neuropathic pain [60-64]. A specific lncRNA, NONRATT021972, was elevated in the blood of diabetic type 2 patients and was found to be positively associated with diabetic neuropathy [65]. LncRNAs were also evaluated in patients with psoriatic arthritis and one particular lncRNA was positively associated with pain [66]. Our study is the first to implicate the identified circulating EV ncRNAs in a neuropathic pain model. Further analysis of the role of EV cargo in the development of neuropathic pain is needed.

Past studies have correlated miRNA and protein expression profiles in human peripheral blood mononuclear cells, linked various diseases to miRNA-protein associations, and highlight the importance of miRNAs interaction with protein networks [67-69]. Further studies indicate that EV miRNA content can affect the targets of interest examined here, including ERK, MAPK, and P70S6K [70-73]. Rat models of neuropathic pain have previously shown increased expression of ERK1/2 and P70S6K [74-77]. Furthermore, several studies have revealed that certain treatments shown to be successful in rodent models of pain, result in reduced ERK1/2 or P70S6K activation [76, 78-86]. Additional mechanistic studies discovered that there is significant cross-talk between ERK1/2 and P70S6K which could contribute to pain formation [87-94]. Further studies should examine the link between EV content and the regulation and contribution of EV cargo targets to neuropathic pain.

One potential therapy for pain is the MSC derived secretome. The MSC secretome has shown analgesic activity in several animal pain models, including diabetic neuropathy, osteoarthritis, partial sciatic nerve ligation, rheumatoid arthritis, and intervertebral disc degeneration [31-33, 95, 96]. These studies indicated the potential for the MSC secretome to treat and reduce nociceptive behavior. Recent studies have also indicated that the positive effects attributed to the secretome are, in part, due to EVs and MSC-EVs/secretome are currently being studied in multiple clinical trials [97, 98]. However, more evidence is required to fully verify the secretome's efficacy and safety in multiple animal models of pain. The secretome evaluated here has been shown previously to reduce brain injury as a result of stroke, diminish inflammation, and stimulate regeneration and repair of brain tissues [43-47]. The secretome or cell-free biologic have specific advantages as a pain therapeutic as opposed to utilizing adult stem cells. The secretome has the potential to be lyophilized and does not require liquid nitrogen storage or special transport conditions. These differences enable cell-free biologics to be more conducive to battlefield use. This current study is the first to reveal this MSC secretome's potential in treating and reducing nociceptive behavior.

Biomarkers serve different roles when used on the battlefield as opposed to the clinic. Injury and pain biomarkers can contribute to evidence based triage and evacuation decisions as well as conservation of limited analgesics. In contrast, such biomarkers used in the clinic can function to promote evidence-based diagnoses. Both of these biomarker roles are essential to quality healthcare. From this and other published research, we can conclude that EV ncRNAs play important roles in injury-induced pain and therefore may function as key injury and/or pain biomarkers.

This study provides novel pain therapeutic targets and pathways and exploiting such pathways may lead to pain reduction.

5. Conclusion

Key findings of this research include, (1) circulating EV-ncRNAs are DE post-nerve injury, (2) p-P70S6K and p-ERK1 are increased in the dorsal PFC at 15 days post-nerve injury, and (3) bath application of the secretome rescues nerve-injury induced mechanical allodynia. These data, along with previously published literature, highlight the critical role that EVs and the secretome may play under normal physiological or pathological conditions. EVs and the secretome have potential as key regulators, biomarkers, and therapeutics.

Appendix

Table A1. *DE EV snoRNAs using both the RNAcentral ID and correlating Ensembl ID.*

RNAcentral ID	Ensembl ID
snoRNAs	**snoRNAs**
URS000071F51C_10116	SNORD50B
URS0000716869_10116	SNORD115
URS00006A1274_10116	SNORD21
URS00006FE715_10116	snoMBII-202
URS0000710B5C_10116	SNORD71
URS0000660107_10116	snoRNA U3
URS0000A84E92_10116	SNORD29
URS0000684D1D_10116	SNORD44
URS00006C30AB_10116	SNORA3
URS0000A8E679_10116	SNORA73
URS000070660D_10116	SNORD95
URS000071DE45_10116	SNORD60
URS000069E108_10116	SNORA16
URS0000636BFB_10116	SNORD73
URS000068F621_10116	snoU83B
URS0000637625_10116	SNORD38
URS00006C10DC_10116	SNORD69
URS000067E7C0_10116	SNORD10

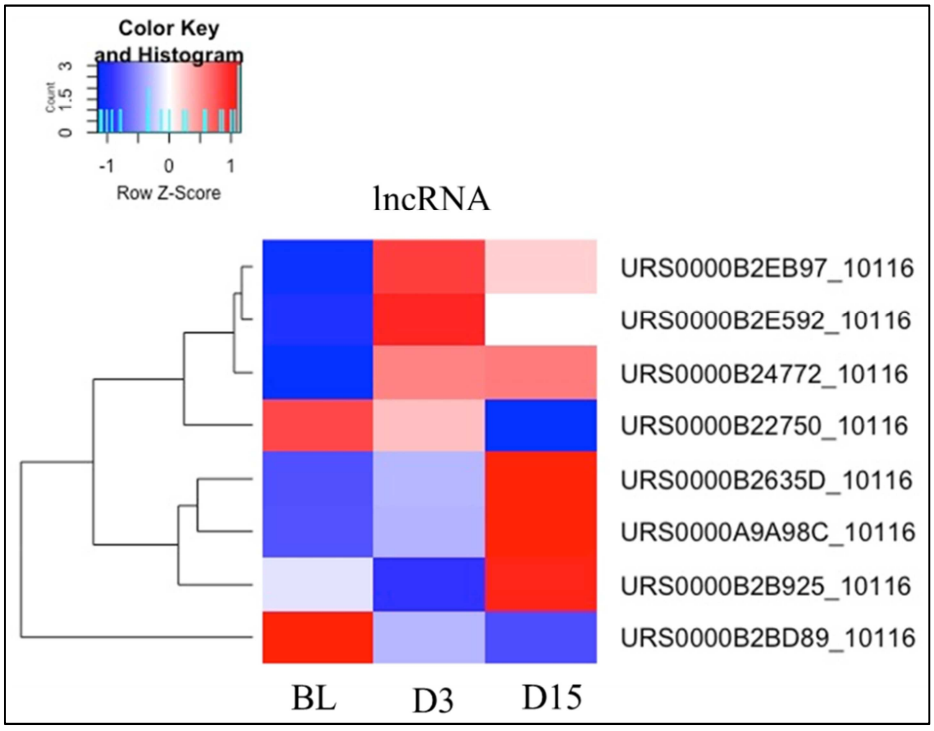

Figure A1. *Heat map highlighting 8 lncRNAs differentially expressed at days 3 and 15 post-SNL. Red: upregulated; blue: downregulated. N=6/group/timepoint.*

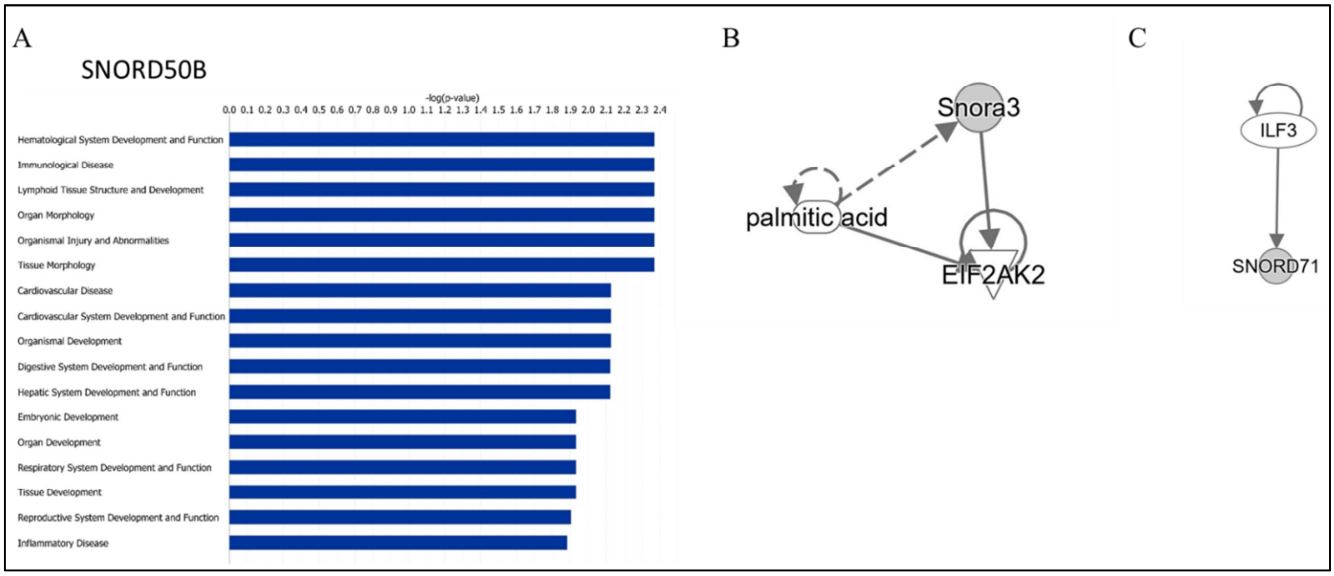

Figure A2. *The Ingenuity pathway analysis (IPA) bioinformatics analysis platform had limited information on the identified EV ncRNAs. Specifically, only SNORD50B was implicated in specific disease functions and SNORD71 and SNORA3 were mapped to known signaling pathways.*

Disclosure

The authors declare no competing financial interests.

DOD Disclaimer

The views expressed in this article are those of the author(s) and do not reflect the official policy or position of the U.S. Army Medical Department, Department of the Army, DOD, or the U.S. Government.

Funding

This research was supported by Congressionally Directed Medical Research Programs-Applied Pain Research (MR157005C) and Combat Casualty Care Research Program (CCCRP, MR190014).

References

[1] Sosanya, N. M., et al., Identifying Plasma Derived Extracellular Vesicle (EV) Contained Biomarkers in the Development of Chronic Neuropathic Pain. J Pain, 2019.

[2] van Niel, G., G. D'Angelo, and G. Raposo, Shedding light on the cell biology of extracellular vesicles. Nat Rev Mol Cell Biol, 2018. *19* (4): p. 213-228.

[3] Keshtkar, S., N. Azarpira, and M. H. Ghahremani, Mesenchymal stem cell-derived extracellular vesicles: novel frontiers in regenerative medicine. Stem Cell Res Ther, 2018. *9* (1): p. 63.

[4] Urabe, F., et al., Extracellular vesicles as biomarkers and therapeutic targets for cancer. Am J Physiol Cell Physiol, 2020. *318* (1): p. C29-C39.

[5] Hill, A. F., Extracellular Vesicles and Neurodegenerative Diseases. J Neurosci, 2019. *39* (47): p. 9269-9273.

[6] Harrell, C. R., et al., Mesenchymal Stem Cell-Derived Exosomes and Other Extracellular Vesicles as New Remedies in the Therapy of Inflammatory Diseases. Cells, 2019. *8* (12).

[7] Kharaziha, P., et al., Tumor cell-derived exosomes: a message in a bottle. Biochim Biophys Acta, 2012. *1826* (1): p. 103-11.

[8] Palazzo, A. F. and E. S. Lee, Non-coding RNA: what is functional and what is junk? Front Genet, 2015. *6*: p. 2.

[9] Liu, Y., et al., The emerging role of the piRNA/piwi complex in cancer. Mol Cancer, 2019. *18* (1): p. 123.

[10] Bachellerie, J. P., J. Cavaille, and A. Huttenhofer, The expanding snoRNA world. Biochimie, 2002. *84* (8): p. 775-90.

[11] Jutzi, D., et al., Aberrant interaction of FUS with the U1 snRNA provides a molecular mechanism of FUS induced amyotrophic lateral sclerosis. Nat Commun, 2020. *11* (1): p. 6341.

[12] Long, Y., et al., How do lncRNAs regulate transcription? Sci Adv, 2017. *3* (9): p. eaao2110.

[13] Chan, J. J. and Y. Tay, Noncoding RNA: RNA Regulatory Networks in Cancer. Int J Mol Sci, 2018. *19* (5).

[14] Carpenter, S., et al., A long noncoding RNA mediates both activation and repression of immune response genes. Science, 2013. *341* (6147): p. 789-92.

[15] Luarte, A., et al., Potential Therapies by Stem Cell-Derived Exosomes in CNS Diseases: Focusing on the Neurogenic Niche. Stem Cells Int, 2016. *2016*: p. 5736059.

[16] Lugli, G., et al., Plasma Exosomal miRNAs in Persons with and without Alzheimer Disease: Altered Expression and Prospects for Biomarkers. PLoS One, 2015. *10* (10): p. e0139233.

[17] Van Giau, V. and S. S. An, Emergence of exosomal miRNAs as a diagnostic biomarker for Alzheimer's disease. J Neurol Sci, 2016. *360*: p. 141-52.

[18] Wickman, J. R., et al., Circulating microRNAs from the mouse tibia fracture model reflect the signature from patients with complex regional pain syndrome. Pain Rep, 2021. *6* (3): p. e950.

[19] Jean-Toussaint, R., et al., Therapeutic and prophylactic effects of macrophage-derived small extracellular vesicles in the attenuation of inflammatory pain. Brain Behav Immun, 2021. *94*: p. 210-224.

[20] Hornick, N. I., et al., Serum Exosome MicroRNA as a Minimally-Invasive Early Biomarker of AML. Sci Rep, 2015. *5*: p. 11295.

[21] Schwarzenbach, H., The clinical relevance of circulating, exosomal miRNAs as biomarkers for cancer. Expert Rev Mol Diagn, 2015. *15* (9): p. 1159-69.

[22] Johnson, L. R., et al., The immunostimulatory RNA RN7SL1 enables CAR-T cells to enhance autonomous and endogenous immune function. Cell, 2021. *184* (19): p. 4981-4995 e14.

[23] Pinho, A. G., et al., Cell Secretome: Basic Insights and Therapeutic Opportunities for CNS Disorders. Pharmaceuticals (Basel), 2020. *13* (2).

[24] Agrawal, G. K., et al., Plant secretome: unlocking secrets of the secreted proteins. Proteomics, 2010. *10* (4): p. 799-827.

[25] Baraniak, P. R. and T. C. McDevitt, Stem cell paracrine actions and tissue regeneration. Regen Med, 2010. *5* (1): p. 121-43.

[26] Hathout, Y., Approaches to the study of the cell secretome. Expert Rev Proteomics, 2007. *4* (2): p. 239-48.

[27] Tjalsma, H., et al., Signal peptide-dependent protein transport in Bacillus subtilis: a genome-based survey of the secretome. Microbiol Mol Biol Rev, 2000. *64* (3): p. 515-47.

[28] Vizoso, F. J., et al., Mesenchymal Stem Cell Secretome: Toward Cell-Free Therapeutic Strategies in Regenerative Medicine. Int J Mol Sci, 2017. *18* (9).

[29] Gnecchi, M., et al., Paracrine action accounts for marked protection of ischemic heart by Akt-modified mesenchymal stem cells. Nat Med, 2005. *11* (4): p. 367-8.

[30] Teixeira, F. G., et al., Secretome of mesenchymal progenitors from the umbilical cord acts as modulator of neural/glial proliferation and differentiation. Stem Cell Rev Rep, 2015. *11* (2): p. 288-97.

[31] Brini, A. T., et al., Therapeutic effect of human adipose-derived stem cells and their secretome in experimental diabetic pain. Sci Rep, 2017. *7* (1): p. 9904.

[32] Khatab, S., et al., Mesenchymal stem cell secretome reduces pain and prevents cartilage damage in a murine osteoarthritis model. Eur Cell Mater, 2018. *36*: p. 218-230.

[33] Gama, K. B., et al., Conditioned Medium of Bone Marrow-Derived Mesenchymal Stromal Cells as a Therapeutic Approach to Neuropathic Pain: A Preclinical Evaluation. Stem Cells Int, 2018. *2018*: p. 8179013.

[34] Diomede, F., et al., Functional Relationship between Osteogenesis and Angiogenesis in Tissue Regeneration. Int J Mol Sci, 2020. *21* (9).

[35] Lee, S. and L. E. Goldfinger, RLIP76 regulates HIF-1 activity, VEGF expression and secretion in tumor cells, and secretome transactivation of endothelial cells. FASEB J, 2014. *28* (9): p. 4158-68.

[36] Asthana, A., et al., Secretome-Based Prediction of Three-Dimensional Hepatic Microtissue Physiological Relevance. ACS Biomater Sci Eng, 2020. *6* (1): p. 587-596.

[37] Rong, X., et al., Human fetal skin-derived stem cell secretome enhances radiation-induced skin injury therapeutic effects by promoting angiogenesis. Stem Cell Res Ther, 2019. *10* (1): p. 383.

[38] Salgado, A. J., et al., Adipose tissue derived stem cells secretome: soluble factors and their roles in regenerative medicine. Curr Stem Cell Res Ther, 2010. *5* (2): p. 103-10.

[39] Khaibullina, A. A., J. M. Rosenstein, and J. M. Krum, Vascular endothelial growth factor promotes neurite maturation in primary CNS neuronal cultures. Brain Res Dev Brain Res, 2004. *148* (1): p. 59-68.

[40] Guaiquil, V. H., et al., VEGF-B selectively regenerates injured peripheral neurons and restores sensory and trophic functions. Proc Natl Acad Sci U S A, 2014. *111* (48): p. 17272-7.

[41] Sosanya, N. M., et al., Involvement of brain-derived neurotrophic factor (BDNF) in chronic intermittent stress-induced enhanced mechanical allodynia in a rat model of burn pain. BMC Neurosci, 2019. *20* (1): p. 17.

[42] Eaton, S. L., et al., Total protein analysis as a reliable loading control for quantitative fluorescent Western blotting. PLoS One, 2013. *8* (8): p. e72457.

[43] Fontanilla, C. V., et al., Adipose-derived Stem Cell Conditioned Media Extends Survival time of a mouse model of Amyotrophic Lateral Sclerosis. Sci Rep, 2015. *5*: p. 16953.

[44] Prochazka, V., et al., Therapeutic Potential of Adipose-Derived Therapeutic Factor Concentrate for Treating Critical Limb Ischemia. Cell Transplant, 2016. *25* (9): p. 1623-1633.

[45] Wei, X., et al., IFATS collection: The conditioned media of adipose stromal cells protect against hypoxia-ischemia-induced brain damage in neonatal rats. Stem Cells, 2009. *27* (2): p. 478-88.

[46] Wei, X., et al., Adipose stromal cells-secreted neuroprotective media against neuronal apoptosis. Neurosci Lett, 2009. *462* (1): p. 76-9.

[47] Zhao, L., et al., Adipose stromal cells-conditional medium protected glutamate-induced CGNs neuronal death by BDNF. Neurosci Lett, 2009. *452* (3): p. 238-40.

[48] Sweeney, B. A., et al., Exploring Non-Coding RNAs in RNAcentral. Curr Protoc Bioinformatics, 2020. *71* (1): p. e104.

[49] Siprashvili, Z., et al., The noncoding RNAs SNORD50A and SNORD50B bind K-Ras and are recurrently deleted in human cancer. Nat Genet, 2016. *48* (1): p. 53-8.

[50] Braicu, C., et al., The Function of Non-Coding RNAs in Lung Cancer Tumorigenesis. Cancers (Basel), 2019. *11* (5).

[51] Mannoor, K., et al., Small nucleolar RNA signatures of lung tumor-initiating cells. Mol Cancer, 2014. *13*: p. 104.

[52] Liu, J., et al., Identification of potential prognostic small nucleolar RNA biomarkers for predicting overall survival in patients with sarcoma. Cancer Med, 2020. *9* (19): p. 7018-7033.

[53] Toms, D., et al., Small RNA sequencing reveals distinct nuclear microRNAs in pig granulosa cells during ovarian follicle growth. J Ovarian Res, 2021. *14* (1): p. 54.

[54] Fitz, N. F., et al., Small nucleolar RNAs in plasma extracellular vesicles and their discriminatory power as diagnostic biomarkers of Alzheimer's disease. Neurobiol Dis, 2021. *159*: p. 105481.

[55] Lee, E. J., et al., Identification of piRNAs in the central nervous system. RNA, 2011. *17* (6): p. 1090-9.

[56] Phay, M., H. H. Kim, and S. Yoo, Analysis of piRNA-Like Small Non-coding RNAs Present in Axons of Adult Sensory Neurons. Mol Neurobiol, 2018. *55* (1): p. 483-494.

[57] Plestilova, L., et al., Expression and Regulation of PIWIL-Proteins and PIWI-Interacting RNAs in Rheumatoid Arthritis. PLoS One, 2016. *11* (11): p. e0166920.

[58] Zhang, C., et al., PiRNA-DQ541777 Contributes to Neuropathic Pain via Targeting Cdk5rap1. J Neurosci, 2019. *39* (45): p. 9028-9039.

[59] Spinelli, C., et al., Extracellular Vesicles as Conduits of Non-Coding RNA Emission and Intercellular Transfer in Brain Tumors. Noncoding RNA, 2018. *5* (1).

[60] Zhou, J., Y. Fan, and H. Chen, Analyses of long non-coding RNA and mRNA profiles in the spinal cord of rats using RNA sequencing during the progression of neuropathic pain in an SNI model. RNA Biol, 2017. *14* (12): p. 1810-1826.

[61] Mao, P., et al., Transcriptomic differential lncRNA expression is involved in neuropathic pain in rat dorsal root ganglion after spared sciatic nerve injury. Braz J Med Biol Res, 2018. *51* (10): p. e7113.

[62] Baskozos, G., et al., Comprehensive analysis of long noncoding RNA expression in dorsal root ganglion reveals cell-type specificity and dysregulation after nerve injury. Pain, 2019. *160* (2): p. 463-485.

[63] Jiang, B. C., et al., Identification of lncRNA expression profile in the spinal cord of mice following spinal nerve ligation-induced neuropathic pain. Mol Pain, 2015. *11*: p. 43.

[64] Zhou, J., et al., Identification of the Spinal Expression Profile of Non-coding RNAs Involved in Neuropathic Pain Following Spared Nerve Injury by Sequence Analysis. Front Mol Neurosci, 2017. *10*: p. 91.

[65] Yu, W., et al., LncRNA NONRATT021972 Was Associated with Neuropathic Pain Scoring in Patients with Type 2 Diabetes. Behav Neurol, 2017. *2017*: p. 2941297.

[66] Yue, T., et al., Comprehensive analyses of long non-coding RNA expression profiles by RNA sequencing and exploration of their potency as biomarkers in psoriatic arthritis patients. BMC Immunol, 2019. *20* (1): p. 28.

[67] Mork, S., et al., Protein-driven inference of miRNA-disease associations. Bioinformatics, 2014. *30* (3): p. 392-7.

[68] Huang, L., F. Y. Deng, and S. F. Lei, Global correlation analysis for miRNA and protein expression profiles in human peripheral blood mononuclear cells. Mol Biol Rep, 2020. *47* (7): p. 5295-5304.

[69] Alshalalfa, M., miRNA regulation in the context of functional protein networks: principles and applications. Wiley Interdiscip Rev Syst Biol Med, 2014. *6* (2): p. 189-99.

[70] Pizzicannella, J., et al., Engineered Extracellular Vesicles From Human Periodontal-Ligament Stem Cells Increase VEGF/VEGFR2 Expression During Bone Regeneration. Front Physiol, 2019. *10*: p. 512.

[71] Jin, Q., et al., Extracellular vesicles derived from human dental pulp stem cells promote osteogenesis of adipose-derived stem cells via the MAPK pathway. J Tissue Eng, 2020. *11*: p. 2041731420975569.

[72] Ma, Y., et al., Induced neural progenitor cells abundantly secrete extracellular vesicles and promote the proliferation of neural progenitors via extracellular signal-regulated kinase pathways. Neurobiol Dis, 2019. *124*: p. 322-334.

[73] Zhou, D., W. Zhai, and M. Zhang, Mesenchymal stem cell-derived extracellular vesicles promote apoptosis in RSC96 Schwann cells through the activation of the ERK pathway. Int J Clin Exp Pathol, 2018. *11* (11): p. 5157-5170.

[74] Song, X. S., et al., Activation of ERK/CREB pathway in spinal cord contributes to chronic constrictive injury-induced neuropathic pain in rats. Acta Pharmacol Sin, 2005. *26* (7): p. 789-98.

[75] Joo, J. D., et al., Lidocaine suppresses the increased extracellular signal-regulated kinase/cyclic AMP response element-binding protein pathway and pro-inflammatory cytokines in a neuropathic pain model of rats. Eur J Anaesthesiol, 2011. *28* (2): p. 106-11.

[76] Guo, J. R., et al., Effect and mechanism of inhibition of PI3K/Akt/mTOR signal pathway on chronic neuropathic pain and spinal microglia in a rat model of chronic constriction injury. Oncotarget, 2017. *8* (32): p. 52923-52934.

[77] Kiguchi, N., et al., Vascular endothelial growth factor signaling in injured nerves underlies peripheral sensitization in neuropathic pain. J Neurochem, 2014. *129* (1): p. 169-78.

[78] Kim, Y., et al., Amitriptyline inhibits the MAPK/ERK and CREB pathways and proinflammatory cytokines through A3AR activation in rat neuropathic pain models. Korean J Anesthesiol, 2019. *72* (1): p. 60-67.

[79] Lin, J. P., et al., Dexmedetomidine Attenuates Neuropathic Pain by Inhibiting P2X7R Expression and ERK Phosphorylation in Rats. Exp Neurobiol, 2018. *27* (4): p. 267-276.

[80] Ji, R. R., et al., MAP kinase and pain. Brain Res Rev, 2009. *60* (1): p. 135-48.

[81] Xu, X., et al., Microglial BDNF, PI3K, and p-ERK in the Spinal Cord Are Suppressed by Pulsed Radiofrequency on Dorsal Root Ganglion to Ease SNI-Induced Neuropathic Pain in Rats. Pain Res Manag, 2019. *2019*: p. 5948686.

[82] Wang, B., et al., PKM2 is involved in neuropathic pain by regulating ERK and STAT3 activation in rat spinal cord. J Headache Pain, 2018. *19* (1): p. 7.

[83] Choi, S., et al., mTOR signaling intervention by Torin1 and XL388 in the insular cortex alleviates neuropathic pain. Neurosci Lett, 2020. *718*: p. 134742.

[84] Tateda, S., et al., Rapamycin suppresses microglial activation and reduces the development of neuropathic pain after spinal cord injury. J Orthop Res, 2017. *35* (1): p. 93-103.

[85] Lopez-Bellido, R., et al., Growth Factor Signaling Regulates Mechanical Nociception in Flies and Vertebrates. J Neurosci, 2019. *39* (30): p. 6012-6030.

[86] Beazley-Long, N., et al., VEGFR2 promotes central endothelial activation and the spread of pain in inflammatory arthritis. Brain Behav Immun, 2018. *74*: p. 49-67.

[87] Cho, Y. R., et al., Broussonetia kazinoki modulates the expression of VEGFR-2 and MMP-2 through the inhibition of ERK, Akt and p70S6K dependent signaling pathways: Its implication in endothelial cell proliferation, migration and tubular formation. Oncol Rep, 2014. *32* (4): p. 1531-6.

[88] Saryeddine, L., et al., EGF-Induced VEGF Exerts a PI3K-Dependent Positive Feedback on ERK and AKT through VEGFR2 in Hematological In Vitro Models. PLoS One, 2016. *11* (11): p. e0165876.

[89] Wang, W., et al., MicroRNA-497 suppresses angiogenesis by targeting vascular endothelial growth factor A through the PI3K/AKT and MAPK/ERK pathways in ovarian cancer. Oncol Rep, 2014. *32* (5): p. 2127-33.

[90] Pengcheng, S., et al., MicroRNA-497 suppresses renal cell carcinoma by targeting VEGFR-2 in ACHN cells. Biosci Rep, 2017. *37* (3).

[91] Zachary, I., Neuroprotective role of vascular endothelial growth factor: signalling mechanisms, biological function, and therapeutic potential. Neurosignals, 2005. *14* (5): p. 207-21.

[92] Ogunshola, O. O., et al., Paracrine and autocrine functions of neuronal vascular endothelial growth factor (VEGF) in the central nervous system. J Biol Chem, 2002. *277* (13): p. 11410-5.

[93] Tovar, Y. R. L. B. and R. Tapia, VEGF protects spinal motor neurons against chronic excitotoxic degeneration in vivo by activation of PI3-K pathway and inhibition of p38MAPK. J Neurochem, 2010. *115* (5): p. 1090-101.

[94] Swendeman, S., et al., VEGF-A stimulates ADAM17-dependent shedding of VEGFR2 and crosstalk between VEGFR2 and ERK signaling. Circ Res, 2008. *103* (9): p. 916-8.

[95] Ferreira, J. R., et al., IL-1beta-pre-conditioned mesenchymal stem/stromal cells' secretome modulates the inflammatory response and aggrecan deposition in intervertebral disc. Eur Cell Mater, 2021. *41*: p. 431-453.

[96] Miranda, J. P., et al., The Secretome Derived From 3D-Cultured Umbilical Cord Tissue MSCs Counteracts Manifestations Typifying Rheumatoid Arthritis. Front Immunol, 2019. *10*: p. 18.

[97] Dabrowska, S., et al., Immunomodulatory and Regenerative Effects of Mesenchymal Stem Cells and Extracellular Vesicles: Therapeutic Outlook for Inflammatory and Degenerative Diseases. Front Immunol, 2020. *11*: p. 591065.

[98] Ghafouri-Fard, S., et al., The Emerging Role of Exosomes in the Treatment of Human Disorders With a Special Focus on Mesenchymal Stem Cells-Derived Exosomes. Front Cell Dev Biol, 2021. *9*: p. 653296.